ISSN 1814-4225 (print)
ISSN 2663-2012 (online)

UDC 621.793.74:620.3-047.58 **doi: 10.32620/aktt.2024.3.06**

Yurii SHYROKYI, Iurii SYSOIEV, Yevhen FESENKO

National Aerospace University "Kharkiv Aviation Institute", Kharkiv, Ukraine

MODELING THE CONDITIONS FOR OBTAINING NANOSTRUCTURES DURING ION-PLASMA PROCESSING TAKING INTO ACCOUNT THE QUANTUM-MECHANICAL PROPERTIES OF ELECTRODE MATERIAL

*The **subject matter** of the article is the thermophysical and mechanical properties of surface layers of structural materials using a quantum-mechanical approach. The **aim** of the article is to adjust the parameters of the heat conductivity and thermoelasticity problem, considering all possible external and internal thermal effects and the quantum-mechanical description of the material structure, for electrodes in vacuum-arc nanostructuring. The **task** to be solved is to perform calculations using the developed model for a copper cathode considering the energy spent on the formation of nanoparticles during ion-plasma processing with oxygen ions. The **methods** used are methods for solving nonlinear problems. The following **results** were obtained. 1. The nature of the dependencies of the maximum temperature, the expected volume of nanostructures, and the maximum depth of their formation on the energy of oxygen ions with charges z = 1 and z = 2 matches previously known dependencies obtained by the classical model, but under quantum-mechanical consideration, the maximum temperature values increase by 15%, the volume of the nanocluster increases by 50%, and the maximum depth of its occurrence increases by 1.5 times. 2. When selecting the parameters of ion-plasma processing for obtaining nanostructures with ion energies 100...500 eV, the previously proposed model with general thermophysical and mechanical properties of structural materials can be used. 3. For technologies with ion energies in the range of 10^3...$2 \cdot 10^3$ eV, the previously proposed model can be used but with quantum-mechanical effects of structural materials considered. 4) For technologies with ion energies above 10^4 eV, calculations should be performed using both approaches (the classical approach and the approach considering the quantum-mechanical properties of structural materials), and after comparison, the variant whose calculation results are closest to the experimental results should be used. **Conclusions**. The proposed theoretical model using the thermophysical, mechanical, and quantum-mechanical properties of structural materials can be used to adjust the technological parameters of ion-plasma processing to assess the formation of nanostructures in protective and strengthening coatings.*

Keywords: *ions; electrons; thermal conductivity; heat capacity; nanostructures; ion energy.*

1. Introduction

1.1. Motivation

In modern production, nanotechnologies are used very widely, for example, as protective coatings for gears and camshafts [1, 2] or as catalysts for chemical reactions [3]. Their use in electronics and microelectronics is no less attractive, for instance, as coatings for electromagnetic waves shielding [4] or as field emission electron sources in vacuum electronics [5], as well as in sensor, electronic, and optoelectronic nanodevices [6].

Nanostructured materials can be obtained using various biosynthetic [7], electrochemical [8], plasma [6], and other methods. Particularly interesting are vacuum-arc methods, which can be used to create thin surface [9, 10] or multilayer nanostructures [11]. They can also be employed for modifying the surface layers of materials [12, 13]. To further expand the use of vacuum-arc nanotechnologies, various scientific studies are constantly being conducted [14, 15]. For instance, in work [16] the influence of changing valence ions at different discharge frequencies in a microcathode arc engine was investigated. Some optical, nanomechanical [17], and physical [18, 19] properties of thin nanostructures were also studied. A lot of works focuses on the creation of nanostructures on materials surfaces [8 – 10], but significantly fewer studies examine the process of their formation in the surface layers and the depth of the material [11, 20].

1.2. State of the art

The main theoretical studies for obtaining nanostructures in structural materials using ion-plasma technologies [21 – 23] are based on the use of thermal conductivity, thermoelasticity, and general material characteristics [24, 25]. However, these methods do not

account for the peculiarities of electronic thermal conductivity and material lattice thermal conductivity (phonon-phonon thermal conductivity), so they may incorrectly consider the dependencies of the coefficient of linear expansion, the modulus of elasticity, the heat capacity, and other physico-mechanical characteristics of the material on the nature of thermal and mechanical impacts. Therefore, it is advisable to address the issue of thermal conductivity and thermoelasticity, taking into account all possible external and internal thermal effects and a quantum-mechanical description of the material structure.

1.3. Objectives and the approach

Considering the above, the thermophysical and mechanical characteristics of materials using a quantum-mechanical approach will be examined. Additionally, calculations based on the developed model for a copper cathode, taking into account the energy expended on the formation of nanoparticles during ion-plasma processing with oxygen ions [25], will be performed. This will allow for a more accurate determination of the technological parameters of ion flows for obtaining nanostructures in the processed material.

2. Consideration of the quantum-mechanical properties of the material for obtaining nanostructures

To address the aforementioned task, the electronic heat capacity of metals will be considered. Within the framework of quantum theory, only electrons in states with energies in the kT interval near the Fermi level $E_F = kT_F$ experience thermal excitation [26, 27]. As the material temperature increases from 0 to T, only a fraction of the electrons, approximately $\sim T/T_F$, experience thermal excitation, since this fraction has energies in the upper part of the material energy distribution within the kT interval. Therefore, each of the $n(T/T_F)$ electrons acquires thermal energy of the order of kT, and total energy ΔE of the electrons thermal excitation will be approximately:

$$\Delta E \approx n\left(T/T_F\right)kT. \qquad (1)$$

The total electronic heat capacity of the material is obtained by differentiating energy with respect to temperature:

$$C_V^e = \frac{\partial \Delta E}{\partial T} \approx 2nk\,T/T_F. \qquad (2)$$

From the expression, it can be seen that the electronic heat capacity depends linearly on temperature. Considering that the Fermi temperature T_F is approximately $5\cdot10^4$ K, the magnitude of the electronic heat capacity for monovalent metals can be estimated. The magnitude C_V^e at room temperature turns out to be approximately one hundred times less than the classical value (3R/2).

For more accurate calculations, the following expression for the electronic heat capacity is used:

$$C_V^e = \pi^2 nk^2 T/2E_F = \pi^2 RT/2T_F = \lambda T, \qquad (3)$$

where λ is the electronic heat capacity coefficient.

Since the lattice heat capacity decreases according to the T^3 law [26], at relatively low temperatures, the electronic component of the heat capacity becomes greater than the lattice component. As a result, at a certain threshold temperature, the electronic contribution to the heat capacity of metals will always prevail. The estimation of this temperature can be conducted by direct comparison of the expressions for the lattice and electronic heat capacities, which for $T_D \cong 300K$ (the Debye temperature) and $T_F = 5\cdot10^4$ K yields a value of around 3~4 K, corresponding to $T/T_D \cong 0.01$. At higher temperatures, the heat capacity is predominantly determined by the lattice (phonon) contribution. At temperatures much lower than T_D, the heat capacity of metals can be represented as the sum of two terms, one representing the contribution of electrons and the other representing the lattice:

$$C_V = C_{Ve} + C_{Vlat} = \gamma T + \alpha T^3. \qquad (4)$$

It was experimentally established [28, 29] that the temperature dependence of the heat capacity of conduction electrons is indeed linear for most metals. However, the coefficient λ can have a magnitude that significantly differs from the value predicted $\sim 5\cdot10^{-4}\left[J/mol\cdot K^2\right]$ based on formula (3). The discrepancy between the calculated and experimentally determined values of the electronic heat capacity coefficient is due to the derivation of formula (3) being conducted within the framework of free electrons theory without considering the band structure of the energy spectrum of electrons in the crystal.

Therefore, the total heat capacity of the crystal lattice of the material may be determined as followed. To establish the heat capacity of the atomic lattice, it is necessary to define the energy of thermal vibrations of the lattice atoms of a solid body. Assuming that in the

ISSN 1814-4225 (print)
ISSN 2663-2012 (online)

frequency range from ν to ν + Δν there is a certain number of normal oscillations, the dependence of the number of normal oscillations on the frequency can be expressed by a distribution function ζ(ν). Multiplying the number of normal oscillations of lattice atoms by the average energy of a normal oscillation of one atom, the total energy of normal oscillations of the lattice atoms in the frequency range from ν to ν + Δν can be obtained. By integrating this expression over the entire spectrum of normal oscillations, the energy of thermal oscillations of the lattice atoms of a solid body is acquired. However, finding the frequency spectrum ζ(ν) of a real crystal is a very complex and labor-intensive task, so the Debye model [26, 27] is used for the consideration of the lattice heat capacity. To simplify the calculations, Debye proposed to assume that the number of normal oscillations of atoms is not infinite but equal to the number of degrees of freedom, 3n. Thus, the frequency spectrum of oscillations of a real solid body can be regarded as the spectrum of oscillations of a homogeneous elastic medium. Therefore, it was proposed to truncate the oscillations spectrum at a certain maximum cutoff frequency ν_{max}, which is determined under the condition that the total number of normal oscillations equals 3n. The main task of this model is to establish the form of the function ζ(ν). According to Debye theory, this distribution function has the form:

$$\begin{cases} \varsigma(\nu) = \dfrac{9n}{\nu_{max}^3} \cdot \nu^2, \ \text{if} \ \ \nu \le \nu_{max}; \\ \varsigma(\nu) = 0, \ \text{if} \ \ \nu > \nu_{max}. \end{cases} \qquad (5)$$

Then the expression for determining the lattice energy will take the following form:

$$U_{lat} = 9nkT\left(T/T_D\right)^3 \int_0^{x_{max}} x^3 dx/(e^x - 1), \qquad (6)$$

where $x_{max} = h\nu_{max}/kT = T_D/T$ and $T_D = h\nu_{max}/k$ is the Debye characteristic temperature, which marks the maximum displacement of the equilibrium position of the atom oscillations. This means that at this temperature, the coefficient of thermal expansion has its maximum value, and further increase in temperature will not affect the value change of the coefficient of thermal expansion. To find the heat capacity, the equation (6) is differentiated:

$$C_V = \frac{dU_{lat}}{dT} = \\ = 9R\left(T/T_D\right)\int_0^{x_{max}} x^4 e^3 dx \Big/ \left(e^x - 1\right)^2. \qquad (7)$$

The limiting cases of finding the heat capacity at temperatures higher and lower than the Debye temperature should be considered.

For temperatures higher than the Debye temperature, this expression transforms to the following value:

$$U_{lat} = 3RT. \qquad (8)$$

According to classical statistical mechanics, for a system of particles with harmonic interactions, the average total energy of a harmonic oscillator is kT per one degree of freedom. Since one atom has three degrees of freedom, the internal energy of a crystal with n atoms is equal to:

$$U_{lat} = 3nkT. \qquad (9)$$

Thus, the lattice heat capacity at constant volume for temperatures above the Debye temperature can be calculated using the following expression:

$$C_v = 3RT/T = 3R. \qquad (10)$$

It should be noted that this expression is valid for simple substances where the crystal lattice nodes contain similar isolated atoms or ions. In this case, C_v approximates to 25 J/(mol·K). For chemical compounds, this expression takes the form:

$$C_v = 3mR, \qquad (11)$$

where m is the number of atoms in the molecule of the substance.

In practice, the applicability of the Debye approximation is verified by calculating the Debye temperature as a function of temperature and then comparing the theoretical and experimental curves of the heat capacity versus temperature. It is noted in [26, 30] that the temperature range where Debye's approximate T^3 law holds true for real substances is significantly lower than could be assumed from the theory. The greatest discrepancy between Debye's theory and the experiment occurs in solid bodies with complex lattices, because in such cases, the distribution function ζ(ν) has a rather complex form, which differs significantly from (5).

It should be noted that the above analysis of atoms thermal oscillations and the lattice heat capacity was conducted within the harmonic approximation. Therefore, the forces arising from the displacement of an atom from its equilibrium position were considered proportional to the displacement, and the potential energy of the displaced particle was considered proportional to the square of the displacement. This is valid only for low energy oscillations which occur at relatively low temperatures. However, as the temperature increases, the anharmonic nature of particle oscillations in the lat-

tice becomes significant, which is due to the curve asymmetry of the dependence particles interaction energy on the distance between them [26]. To account for the anharmonicity of atoms oscillations, corrections to the heat capacity at high temperatures are used.

As is known, the ability of metals to conduct electric current is associated with the ability of electrons to move freely through the crystal [26]. This indicates that, under normal conditions, electron gas crystallization does not occur in a metal. Thus, it can be assumed that the system of interacting electrons in a metal is an electron liquid composed of Fermi particles. Therefore, it is quite appropriate to determine the energies and velocities of electrons in the crystal lattice.

If there are nz electrons in the crystal (n is the number of atoms, z is their valency), then at a temperature T = 0 K, they are arranged in momentum space in such a way that all lower energy states are filled. That is, at T = 0 K, the electrons fill a sphere in p-space with a radius R_F, which can be determined from the relationship:

$$nz = 2V\frac{4}{3}\pi R_F^3 \Big/ (2\pi d)^3, \qquad (12)$$

then it will look like this:

$$R_F = 2\pi d(3nz/3\pi V)^{\frac{1}{3}} = d\left(3\pi^2 N\right)^{\frac{1}{3}}, \qquad (13)$$

where $N = nz/V$ is the electron density, and d is the Dirac constant.

The distribution of electrons in the crystal over energy levels at any temperature follows Fermi-Dirac statistics, where the probability f_{En} of finding an electron in a state with energy E_n is described by the function:

$$f_{En} = \left(\exp\frac{E_n - \mu}{k_B T} + 1\right)^{-1}, \qquad (14)$$

where μ is the chemical potential and k_B is the Boltzmann constant.

At T = 0 K, the probability of filling all states with energy $E_F > E_n$ is equal to one, while in the state $E_F \le E_n$ it is equal to zero [26]. Thus, the parameter E_n in (14) determines the threshold energy in metals, below which all energy states are filled at T = 0 K, and above which they are empty.

At a final temperature $T \neq 0$ K, the filling boundary is blurred by the order of $k_B T$, so at $E_n = E_F$, f_{En} is equal to ½.

The Fermi energy corresponding to the filling boundary can be found using formula:

$$E_F = R_F^2/2m_0 = \left(d^2/2m_0\right)\left(3\pi^2 nz/V\right)^{\frac{2}{3}}, \qquad (15)$$

where m_0 is the rest mass of a free electron.

The velocity of an electron on the Fermi surface can be found using the following expression:

$$V_F = R_F/m = d\left(3\pi^2 n\right)^{\frac{1}{3}}\Big/m = h\left(3\pi^2\, nz/V\right)^{\frac{1}{3}}\Big/m. \qquad (16)$$

Since $n^{2/3}$, from equation (15), it can be seen that the Fermi energy increases with increasing electron concentration. This is because, in the ideal gas model, the interaction between electrons is not taken into account. In a metal, collective electrons form a system of particles whose Coulomb interaction energy is approximately equal to e^2/r at the average distance between particles $r \sim 1/n^2$, and is of the same order of magnitude as their kinetic energy $\sim R_F^2/2m_e$. In general, the ground state of a Fermi liquid is structureless. The strong interaction between particles in a Fermi liquid means that adding or removing a few particles changes not only the total energy of the system but also the state of all remaining particles in the system. Consequently, electrons forming the Fermi liquid in general are not considered as particles with definite energy and momentum values [28]. Two main postulates of Fermi liquid theory proposed by Landau [27, 28] will be further relied, which state that when electron interactions are included, the classification of electronic states does not change. At the same time, the ground state becomes structureless, and the electrons forming it cannot be considered as quasiparticles. Thus, when transitioning to a Fermi liquid, the radius of the sphere delimiting filled electron states at T = 0 K remains the same and is determined by equation (13), just as in the gas model. Therefore, the states of the Fermi system at low excitation levels can be described as an almost ideal gas [28, 29].

As mentioned above, the lattice thermal conductivity is caused by the anharmonic nature of its atoms oscillations. The occurrence of anharmonic atoms oscillations leads to the loss of independence of the lattice normal oscillations. Consequently, the encountered oscillations interact with each other, exchange energy, and change the direction of their propagation (scattering off each other). As a result of these processes, during the

ISSN 1814-4225 (print)
ISSN 2663-2012 (online)

interaction of elastic waves, the transfer of energy from oscillations of one frequency to oscillations of another frequency becomes possible until a thermal equilibrium is established in the crystal.

Considering the process of scattering of normal oscillations off each other is convenient from the perspective of phonons (quanta of lattice normal oscillations). For this purpose, a thermally excited crystal should be represented as a box filled with phonons. In the harmonic approximation with independent normal lattice oscillations, phonons form an ideal gas (where phonons do not interact). Therefore, the transition to anharmonic oscillations can be represented as interactions between phonons, resulting in processes such as phonon splitting into two or more phonons or the formation of one phonon from two.

In general, heat transfer in an atomic lattice occurs through both phonons and free electrons. Therefore, thermal conductivity in metals consists of conductivity caused by phonons (lattice thermal conductivity) and conductivity caused by free electrons:

$$C_\lambda = C_{\lambda e} + C_{\lambda.lat}. \qquad (17)$$

To find the lattice thermal conductivity, it is considered as a phonon gas. From the kinetic theory of gases [29, 30], the coefficient of gas thermal conductivity is given by:

$$C_g = lC_v V/3, \qquad (18)$$

where l is the free path length of gas molecules, v is the thermal velocity of the gas, and C_v is the heat capacity per unit volume of the gas.

When applying formula (18) to the phonon gas, an expression for the lattice thermal conductivity is obtained:

$$C_{lat} = l_f C_{vf} V_f /3, \qquad (19)$$

where C_{vf} is the heat capacity per unit volume of the crystal (phonon gas), l_f is the free path length of phonons, and V_f is the velocity of phonons (the speed of sound).

The thermal conductivity of the electron gas can be determined using the formula for the thermal conductivity of gases:

$$C_e = l_e C_e V_f /3. \qquad (20)$$

As shown in [26], the thermal conductivity of typical (pure) metals is almost entirely determined by the thermal conductivity of their electron gas, with the lattice thermal conductivity accounting for only a few percent. However, this changes when transitioning to metallic alloys (heterogeneous metals) due to electron scattering on impurity atoms.

To determine the lattice (phonon-phonon) thermal conductivity, accounting for both resistive and normal phonon scattering processes, the Calloway's expression can be used:

$$C_{\lambda.lat} = C_{\lambda..r} + C_{\lambda.n}, \qquad (21)$$

where $C_{\lambda..r} = \frac{k_B}{2\pi^2 V}\left(\frac{k_B}{h}\right)^3 T^3 \int_0^{T_D} \frac{x^4 e^x dx}{\left(\tau_R^{-1} + \tau_N^{-1}\right)\left(e^x - 1\right)^2}$,

$$C_{\lambda.n} = \frac{k_B}{2\pi^2 V}\left(\frac{k_B}{h}\right)^3 T^3 \times$$

$$\times \left(\int_0^{T_D} \frac{\tau_N^{-1} x^4 e^x dx}{\left(\tau_R^{-1} + \tau_N^{-1}\right)\left(e^x - 1\right)^2} \right)^2 \Bigg/ \left(\int_0^{T_D} \frac{\tau_N^{-1}\tau_R^{-1} x^4 e^x dx}{\left(\tau_R^{-1} + \tau_N^{-1}\right)\left(e^x - 1\right)^2} \right),$$

$$x = h\omega/k_B T,$$

k_B is the Boltzmann constant, h is the Planck constant, τ is the total relaxation time, and τ_R is the relaxation time reflecting the contribution to resistive scattering of normal processes.

Since a heterogeneous metal is obtained during ions processing, to determine the thermal expansion, the following expression is used:

$$\alpha = \left(\gamma C_{v.lat} + \frac{2}{3} C_{v.e}\right) \Big/ 3DV, \qquad (22)$$

where D is the bulk modulus, V is the atomic volume, γ is the Grüneisen constant, $C_{v.lat}$ is the lattice heat capacity at constant volume, and $C_{v.e}$ is the electronic heat capacity at constant volume.

Since the Grüneisen constant has a value greater than one, the electronic contribution to the metal thermal expansion is significant only at very low temperatures, of the order of 10 K. Therefore, in isotropic solid bodies, the coefficients of linear expansion are the same in all directions.

To verify the developed model, the effect of oxygen ions in a plasma environment on copper will be considered. Subsequently, using the theoretical model [25], the technological parameters of obtaining nanostructures with both the conventional and the refined thermal conductivities as described in (11) and (21) will be compared.

3. Results and discussion

According to the presented model [25], which incorporates thermophysical, mechanical, and quantum-mechanical characteristics, the technological parameters required for the formation of nanostructures of a certain volume, both in terms of volume and depth, during the processing of copper with oxygen ions were calculated. The obtained results were compared with known experimental data [23, 24] and reference data [23].

As a result of the calculations, a graph was determined showing the dependence of the maximum temperature on the energy of oxygen ions with charges z = 1 and z = 2 (Fig. 1). Additionally, graphs were obtained showing the dependencies of the expected volume of nanostructures and the maximum depth of their formation on the energy of oxygen ions (Figs. 2, 3). It is evident that the nature of the dependencies of the maximum temperature and volume coincides with those in [24]. However, when considering the quantum-mechanical approach, the values of the maximum temperature increase by 15% (Fig. 1), the volume of the nanocluster increases by 50%, and the maximum depth of occurrence increases by 1.5 times (Figs. 2, 3).

A comparison of the results for maximum temperature, nanostructures volume, and depth of their formation, calculated using the classical model [24] and quantum-mechanical theory, with experimental studies [25] showed that for low ion energies (around 500 eV), the differences in results are negligible. However, at energies of $2 \cdot 10^4$ eV, the discrepancy increases significantly, and at an energy of 10^4 eV, the results differ substantially.

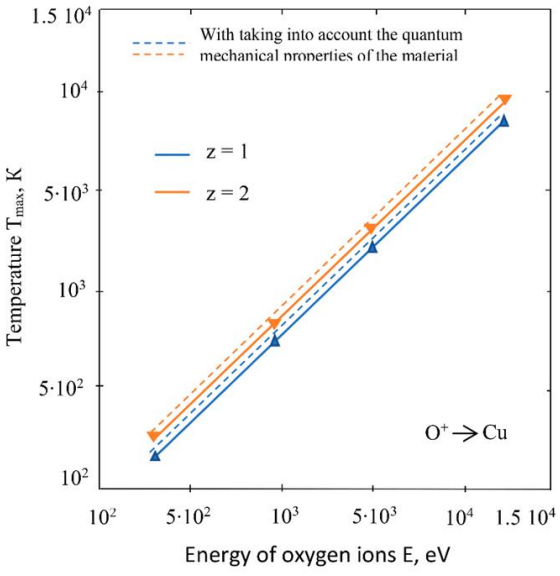

Fig. 1. Dependence of the maximum temperature on the energy of oxygen ions

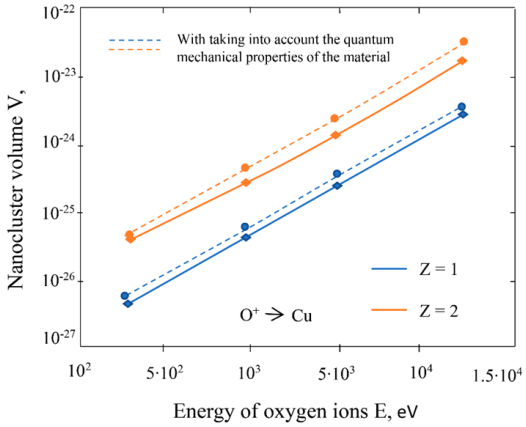

Fig. 2. Dependence of the nanostructure volume on the energy of oxygen ions

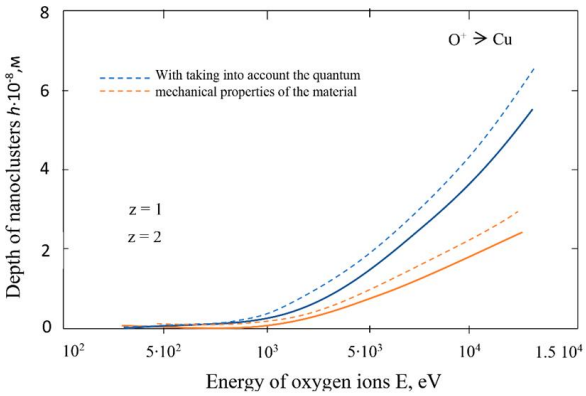

Fig. 3. Dependence of the depth of nanostructures formation on the energy of oxygen ions

All of this indicates that when calculating the parameters for technologies creating nanostructures with ion energies up to 110 eV, it is possible to rely on the classical representation of the physical and mechanical characteristics of materials. However, for energies in the range of 110...500 eV, both classical and quantum-mechanical methods should be used. At the same time, for energies higher than 10^4 eV, it is necessary to evaluate the quantum-mechanical properties of the material. Therefore, for processing methods such as ion implantation and ion doping, calculations should be performed using both classical and quantum-mechanical theories, whereas for plasma processing, the previously proposed model [25] can be used.

4. Conclusions

The study shows that when calculating the parameters of nanostructures for technologies with ion energies 100...500 eV, the previously proposed model with general thermophysical and mechanical characteristics should be used. For ion energies in the range of 10^3...$2 \cdot 10^3$ eV, quantum-mechanical effects need to be

ISSN 1814-4225 (print)
ISSN 2663-2012 (online)

considered when using the same model. For energies above 10^4 eV, calculations should be performed using both classical and quantum-mechanical approaches, and after comparison the calculation results, the option closest to the experimental results should be used. The presented theoretical model can be used to adjust the technological parameters of ion-plasma processing to obtain nanostructures in protective and strengthening coatings.

In the future, it would be appropriate to consider the thermophysical and mechanical properties of the surface layers using the developed model for cathodes made of other materials, especially when obtaining multicomponent coatings.

Contributions of authors: conceptualization, methodology, problem formulation – **Iurii Sysoiev**, model development, verification and analysis of results – **Yurii Shyrokyi**, visualization, review and editing – **Yevhen Fesenko**.

Conflict of interest

The authors declare that they have no conflict of interest in relation to this research, whether financial, personal, authorship, or otherwise, that could affect the research and its results presented in this paper.

Financing

This research was conducted without financial support.

Data availability

The manuscript contains no associated data.

Use of Artificial Intelligence

The authors confirm that they did not use artificial intelligence methods while creating the presented work.

Acknowledgements.

The authors express their gratitude to the National Research Fund of Ukraine for support (competition *"Supporting Research of Leading and Young Scientists"*, project number 2020.02/0119).

All authors have read and agreed to the published version of this manuscript.

References

1. Vladoiu, R., Mandes, A., Dinca, V., Balasoiu, M., Soloviov, D., & Turchenko, V. Synthesis and Characterization of Complex Nanostructured Thin Films Based on Titanium for Industrial Applications. *Materials*, 2020, vol. 13, no. 2, article no. 399. DOI: 10.3390/ma13020399.

2. Kostyuk, G., Popov, V., Shyrokyi, Y., & Yevsieienkova, H. Efficiency and Performance of Milling Using Cutting Tools with Plates of a New Class. *In: Tonkonogyi, V., Ivanov, V., Trojanowska, J., Oborskyi, G., & Pavlenko, I. (eds) Advanced Manufacturing Processes II. InterPartner 2020. Lecture Notes in Mechanical Engineering. Springer, Cham*, 2021, pp. 598-608. DOI: 10.1007/978-3-030-68014-5_58.

3. Jain, M., Yadav, M., & Chaudhry, S. Copper oxide nanoparticles for the removal of divalent nickel ions from aqueous solution, *Toxin Reviews*, 2021, vol. 40, iss. 4, pp. 872-885. DOI: 10.1080/15569543.2020.1799407

4. Wang, C., Murugadoss, V., Kong, J., He, Z., Mai, X., Shao, Q., Chen, Y., Guo, L., Liu, C., Angaiah, S., & Guo, Z. Overview of carbon nanostructures and nanocomposites for electromagnetic wave shielding. *Carbon*, 2018, vol. 140, pp. 696-733. DOI: 10.1016/j.carbon.2018.09.006.

5. Giubileo, F., Di Bartolomeo, A., Iemmo, L., Luongo, G., Urban, & F. Field Emission from Carbon Nanostructures, *Applied Sciences*, 2018, vol. 8, iss. 4, article no. 526. DOI: 10.3390/app8040526.

6. Jafari, A., Tahani, K., Dastan, D., Asgary, S., Shi, Z., Yin, X.-T., Zhou, W.-D., Garmestani, H., & Ţălu, Ş. Ion implantation of copper oxide thin films; statistical and experimental results. *Surfaces and Interfaces*, 2020, vol. 18, article no. 100463. DOI: 10.1016/j.surfin.2020.100463.

7. Sreeju, N., Rufus, A., & Daizy P. Studies on catalytic degradation of organic pollutants and antibacterial property using biosynthesized CuO nanostructures. *Journal of Molecular Liquids*, 2017, vol. 242, pp. 690-700. DOI: 10.1016/j.molliq.2017.07.077.

8. Khan, M. A., Mahmood, H., Khan, M. S., Iqbal, T., Ahmad, P., Shafique, M., & Naeem, M. Microplasma-assisted synthesis of CuO nanostructures for catalytic degradation of organic dyes under solar irradiation. *Journal of Solid State Electrochemistry*, 2020, vol. 24, pp. 1123-1132. DOI: 10.1007/s10008-020-04602-5.

9. Košiček, M., Baranov, O., Zavašnik, J., & Cvelbar, U. In search of the limits of CuO thermal oxidation nanowire growth by combining experiment and theory. *Applied Physics Letters*, 2023, vol. 123, article no. 041601. DOI: 10.1063/5.0151293.

10. Dinca-Balan, V., Vladoiu, R., Mandes, A., & Prodan, G. Correlation study of nanocrystalline carbon doped thin films prepared by a thermionic vacuum arc deposition technique. *Journal of Physics D: Applied Physics*, 2017, vol. 50, no. 43, article no. 435305, DOI: 10.1088/1361-6463/aa86dc.

11. Vladoiu, R., Tichý, M., Mandes, A., Dinca, V., & Kudrna, P. Thermionic Vacuum Arc – A Versatile Technology for Thin Film Deposition and Its Applications. *Coatings*, 2020, vol. 10, iss. 3, article no. 211. DOI: 10.3390/coatings10030211.

12. Breus, A., Abashin, S., Lukashov, I., Serdiuk, O., & Baranov, O. Synthesis of Copper Nanoparticles on Graphite Using Transient Glow-to-Arc Dis-

charge Plasma. *In: Tonkonogyi, V., Ivanov, V., Trojanowska, J., Oborskyi, G., & Pavlenko, I. (eds) Advanced Manufacturing Processes IV, InterPartner 2022. Lecture Notes in Mechanical Engineering. Springer, Cham*, 2022, pp. 264-273. DOI: 10.1007/978-3-031-16651-8_25.

13. Kostyk, K., Kostyk, V., Akimov, O., Kamchatna-Stepanova, K., & Shyrokyi, Y. Ensuring the High Strength Characteristics of the Surface Layers of Steel Products. *In: Tonkonogyi, V., Ivanov, V., Trojanowska, J., Oborskyi, G., Pavlenko, I. (eds) Advanced Manufacturing Processes IV, InterPartner 2022. Lecture Notes in Mechanical Engineering. Springer, Cham*, 2022, pp. 292-301. DOI: 10.1007/978-3-030-91327-4_29.

14. Breus, A., Abashin, S., & Serdiuk, O. Formation of 2D Carbon Nanosheets and Carbon-Shelled Copper Nanoparticles in Glow Discharge. *In: Tonkonogyi, V., Ivanov, V., Trojanowska, J., Oborskyi, G., & Pavlenko, I. (eds) Advanced Manufacturing Processes V. InterPartner 2023. Lecture Notes in Mechanical Engineering. Springer, Cham*, 2024, pp. 256-264. DOI: 10.1007/978-3-031-42778-7_23.

15. Kostyuk, G., Nechyporuk, M., & Kostyk, K. Determination of Technological Parameters for Obtaining Nanostructures under Pulse Laser Radiation on Steel of Drone Engine Parts. *10th International Conference on Dependable Systems, Services and Technologies (DESSERT)*, 2019, pp. 208-212. DOI: 10.1109/DESSERT.2019.8770053.

16. Ji, T., Wei, L., Wang, Y., Song, Y., Cai, H., Li, H., Ding, Y., & Yu, D. Influence of pulse frequency on discharge characteristics of micro-cathode arc thruster. *Vacuum*, 2022, vol. 196, article no. 110748. DOI: 10.1016/j.vacuum.2021.110748.

17. Ay, G. M. & Pat, S. Optical and Nanomechanical Properties of C Coated BN Thin Film Deposited by Thermionic Vacuum Arc Technique. *Journal of Solid State Science and Technology*, 2021, vol. 10, no. 10, article no. 103013. DOI: 10.1149/2162-8777/ac2f1f.

18. Elmas, S., Pat, S., Mohammadigharehbagh, R., Musaoğlu, C., Özgür, M., Demirkol, U., Özen, S., & Korkmaz, Ş. Determination of physical properties of graphene doped ZnO (ZnO:Gr) nanocomposite thin films deposited by a thermionic vacuum arc technique. *Physica B: Condensed Matter*, 2019, vol. 557, pp. 27-33. DOI: 10.1016/j.physb.2018.12.039.

19. Vladoiu, R., Mandes, A., Dinca-Balan, V., & Bursikova, V. Structural and Mechanical Properties of Nanostructured C-Ag Thin Films Synthesized by Thermionic Vacuum Arc Method. *Journal of Nanomaterials*, 2018, article no. 9632041, 10 p. DOI: 10.1155/2018/9632041.

20. Baranov, O. O., Fang, J., Rider, A. E., Kumar, S., & Ostrikov, K. Effect of Ion Current Density on the Properties of Vacuum Arc-Deposited TiN Coatings. *IEEE Transactions on Plasma Science*, 2013, vol. 41, no. 12, pp. 3640–3644. DOI: 10.1109/TPS.2013.2286405.

21. Baranov, O., Romanov, M., Fang, J., Cvelbar, U., & Ostrikov, K. Control of ion density distribution by magnetic traps for plasma electrons. *Journal of Applied Physics*, 2012, vol. 112, no. 7, article no. 073302. DOI: 10.1063/1.4757022.

22. Schmool, D. *Nanotechnologies: The Physics of Nanomaterials. Volume I: The Physics of Surfaces and Nanofabrication Techniques*. 1st ed. Apple Academic Press Publ., 2021. 420 p. DOI: 10.1201/9781003100218.

23. Cao, G., & Wang Y. *Nanostructures and Nanomaterials. Synthesis, Properties, and Applications.* 2nd ed. World Scientific Publishing, 2011. 596 p. DOI: 10.1142/7885.

24. Kostyuk, G., Popov, V., & Kostyk, K. Volume of the Nanocluster and Its Depth at Effect of Ions of Different Energies, Varieties and Charges on Titanium Alloy VT-1. *In: Tonkonogyi, V., Ivanov, V., Trojanowska, J., Oborskyi, G., & Pavlenko, I. (eds) Advanced Manufacturing Processes. InterPartner 2019. Lecture Notes in Mechanical Engineering. Springer, Cham*, 2020, pp. 415-423. DOI: 10.1007/978-3-030-40724-7_42.

25. Kostyuk, G., Melkoziorova, O., Kostyuk, E., & Shirokiy, I. Prospects for producing nanostructures in the volume of parts under the action of plasma flows. *Cutting & Tools in Technological Systems*, 2020, no. 92, pp. 107-121. DOI: 10.20998/2078-7405.2020.92.12

26. Fulde, P., & Jensen, J. Electronic heat capacity of the rare-earth metals. *American Physical Society Phys. Rev. B*, 1983, vol. 27, iss. 7, article no. 4085. DOI: 10.1103/PhysRevB.27.4085.

27. Stauber, T., Peres, N. M. R., Guinea, F., & Castro Neto, A. H. Fermi liquid theory of a Fermi ring. *American Physical Society Phys. Rev. B*, 2007, vol. 75, iss. 11, article no. 115425. DOI: 10.1103/PhysRevB.75.115425.

28. Baym, G., & Pethick, C. *Landau Fermi-Liquid Theory: Concepts and Applications*. John Wiley & Sons, 2007. 211 p.

29. Grad, H. Principles of the Kinetic Theory of Gases. *In: Flügge S. (eds) Thermodynamik der Gase / Thermodynamics of Gases. Handbuch der Physik / Encyclopedia of Physics.* Springer, Berlin, Heidelberg, 1958, vol. 3/12, pp. 205-294. DOI: 10.1007/978-3-642-45892-7_3.

30. Wölfle, P. Quasiparticles in condensed matter systems. *Reports on Progress in Physics*, 2018, vol. 81, no. 3, article no. 032501. DOI: 10.1088/1361-6633/aa9bc4.

Надійшла до редакції 11.05.2024, розглянута на редколегії 15.06.2024.

ISSN 1814-4225 (print)
ISSN 2663-2012 (online)

МОДЕЛЮВАННЯ УМОВ ОТРИМАННЯ НАНОСТРУКТУР ПРИ ІОННО-ПЛАЗМОВІЙ ОБРОБЦІ З УРАХУВАННЯМ КВАНТОВО-МЕХАНІЧНИХ ВЛАСТИВОСТЕЙ МАТЕРІАЛУ ЕЛЕКТРОДІВ

Ю. В. Широкий, Ю. О. Сисоєв, Є. І. Фесенко

Предметом вивчення в статті є теплофізичні та механічні характеристики поверхневих шарів конструкційних матеріалів з використанням квантово-механічного підходу. **Метою** статті є корекція параметрів задачі теплопровідності й термопружності, враховуючи всі можливі зовнішні та внутрішні теплові впливи та квантово-механічний опис будови матеріалу, для електродів при вакуумно-дуговому отриманні наноструктур. **Завдання**: провести розрахунки за розробленою моделлю для мідного катоду з урахуванням енергії, витраченої на утворення наночасток при іонно-плазмовій обробці іонами кисню. Використовуваними **методами** є методи розв'язання нелінійних задач. Отримані наступні **результати**. 1. Характер залежностей максимальної температури, очікуваного об'єму наноструктур і максимальної глибини їх формування від енергії іонів кисню з зарядами z=1 та z=2 збігається з раніше відомими залежностями, отриманими за класичною моделлю, але при квантово-механічному розгляді значення максимальної температури зростають на 15%, об'єм нанокластера зростає на 50%, а максимальна глибина його залягання збільшується у 1.5 рази. 2. При виборі параметрів іонно-плазмової обробки для отримання наноструктур при технологіях з енергіями іонів 100...500 еВ потрібно користуватися раніше запропонованою моделлю з загальними теплофізичними та механічними характеристиками конструкційних матеріалів. 3. При технологіях з енергіями іонів у діапазоні 10^3...$2\cdot10^3$ еВ можна користуватись раніше запропонованою моделлю, але потрібно враховувати квантово-механічні характеристики конструкційних матеріалів. 4. При технологіях з енергіями іонів вище 10^4 еВ необхідно проводити розрахунки за двома варіантами (класичний підхід та підхід з врахуванням квантово-механічних характеристик конструкційних матеріалів) і після порівняння використовувати варіант, результати розрахунків за яким є найближчими до експериментальних результатів. **Висновки**. Наведену теоретичну модель з використанням теплофізичних, механічних і квантово-механічних характеристик конструкційних матеріалів можна використовувати для корегування технологічних параметрів іонно-плазмової обробки з метою оцінки отримання наноструктур в захисних та зміцнюючих покриттях.

Ключові слова: іони; електрони; теплопровідність; теплоємність; наноструктури; енергія іонів.

Широкий Юрій Вячеславович – канд. техн. наук, доц., доц. каф. теоретичної механіки, машинознавства та роботомеханічних систем, Національний аерокосмічний університет ім. М. Є. Жуковського «Харківський авіаційний інститут», Харків, Україна.

Сисоєв Юрій Олександрович – д-р техн. наук, старш. наук. співроб., проф. каф. теоретичної механіки, машинознавства та роботомеханічних систем, Національний аерокосмічний університет ім. М. Є. Жуковського «Харківський авіаційний інститут», Харків, Україна.

Фесенко Євген Ігорович – асп. каф. теоретичної механіки, машинознавства та роботомеханічних систем, Національний аерокосмічний університет ім. М. Є. Жуковського «Харківський авіаційний інститут», Харків, Україна.

Yurii Shyrokyi – PhD, Associate Professor, Department of Theoretical Mechanics, Engineering and Robotic Systems, National Aerospace University "Kharkiv Aviation Institute", Kharkiv, Ukraine,
e-mail: i.shyrokyi@khai.edu, ORCID: 0000-0002-4713-0334, Scopus Author ID: 57222322443.

Iurii Sysoiev – Doctor of Technical Sciences, Professor, Department of Theoretical Mechanics, Engineering and Robotic Systems, National Aerospace University "Kharkiv Aviation Institute", Kharkiv, Ukraine,
e-mail: i.sysoiev@khai.edu, ORCID: 0000-0001-5006-8546.

Yevhen Fesenko – PhD Student, Department of Theoretical Mechanics, Engineering and Robotic Systems, National Aerospace University "Kharkiv Aviation Institute", Kharkiv, Ukraine,
e-mail: y.fesenko@student.csn.khai.edu, ORCID: 0009-0000-4670-4909.